

Short communication

## Lignin-based membranes for electrolyte transference

Xiao Zhang<sup>a</sup>, Juana Benavente<sup>b</sup>, Ricard Garcia-Valls<sup>a,\*</sup>

<sup>a</sup> *Departament d'Enginyeria Química, Escola Tècnica Superior d'Enginyeria Química, Universitat Rovira i Virgili, Av. Països Catalans 26, 43007 Tarragona, Spain*

<sup>b</sup> *Department of Applied Physics, Faculty of Science, University of Málaga, Málaga, Spain*

Accepted 7 February 2005  
Available online 1 June 2005

### Abstract

Homogeneous PSf-LS membranes are formed by incorporating Lignosulfonate (LS) into the Polysulfone (PSf) network. LS obtained from sulfite pulping process contains sulfonic acid groups that will act as proton transport media. PSf-LS membranes were characterized by reflectance Infrared and scanning electron microscopy. LS showed significant influence on membrane morphology. Higher LS concentration caused a decrease in macrovoid formation and induced larger pores. Precipitation temperature was investigated as influencing parameter. Proton fluxes through PSf-LS membranes were measured by transport experiments. Impedance analysis confirmed that PSf-LS membranes possess ion conductivity. The selected PSf-LS membranes exhibited high selectivity for proton over methanol, which indicates their potential applicability in direct methanol fuel cell (DMFC).

© 2005 Elsevier B.V. All rights reserved.

**Keywords:** Lignosulfonate; Polymer blends; Membrane morphology; Proton conductivity; Selectivity

### 1. Introduction

As an alternative energy source, polymer electrolyte membrane fuel cell (PEMFC) has developed quickly since 1980s. Hydrogen fuel cell powered electric buses are already running in Canada and USA. A Japanese company has declaimed that in 2005 they are going to put into market a new type mobile phone powered by direct methanol fuel cell (DMFC). Recently, China is backing up this global event and shows its potential in the PEMFC market.

The most important part of PEMFC is the proton transport membrane. At present, there are only few commercial membranes to meet the market, i.e. Nafion<sup>®</sup> by Du Pont. Nafion is a perfluorosulfonic acid (PFSA)-based polymer. This membrane is still quite expensive. It is commonly used in hydrogen fuel cell. Nafion shows a high methanol cross-over, which limits its application in DMFC due to its consequent lowering of the efficiency, one of the factors in

fuel cell implementation. Under this scenario, materials for proton transport membrane have been developed quickly. Many of them are sulfonated polymers and their blends. For example, sulfonated PSf, sulfonated PEEK, sulfonated polyimide among others. Sulfonation provides sulfonic acid groups in the polymer main chain, which improves the proton transport. Usually the sulfonation degree determines the proton transport of the membrane, high sulfonation degree results in high proton transport [1,2]. On the other hand, high sulfonation degree also increases methanol transport since methanol can be transported by electro-osmotic drag and diffusion [3]. Therefore, an optimized sulfonation degree is crucial to control the membrane property.

Instead of modifying polymers by a sulfonation process, our approach to the problem is the application of lignosulfonate (LS) in the preparation of a proton transport membrane. LS is an amorphous, polyphenolic, high cross-linked polymer containing sulfonic acid groups. Its molecular structure is showed in Fig. 1. LS is a by-product of sulfite pulping. Annually a huge amount of LS is produced all around

\* Corresponding author. Tel.: +34 977 55 96 11; fax: +34 977 55 85 44.  
E-mail address: [ricard.garcia@urv.net](mailto:ricard.garcia@urv.net) (R. Garcia-Valls).

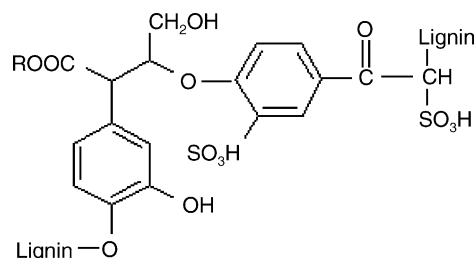


Fig. 1. Molecular structure of LS.

the world. It has application as additive [4], surfactant [5]. LS has also been reported as a component in polymer blends and showed bioactive and biocompatibility [6]. Moreover, LS has applications in blends with thermoplastics [7]. Although LS research is getting more attention, most of LS is incinerated as a waste and it is still a significant environmental burden.

Incorporating LS into PSf matrix to produce membrane provides membrane with proton-affiliated functional groups. The preparation procedure of the membrane can be simple and industry compatible. The membrane price would easily be lower than the commercially available at present. This new exploration of LS application could be of significant improvement from both the economical and environmental point of view.

## 2. Experimental

### 2.1. Preparation of PSf-LS membranes

PSf ( $M_w$  35,000) was purchased from Aldrich and LS ( $7000 \text{ g mol}^{-1}$ ) was provided by Lignotech. The casting solution was prepared by dissolving LS and 15 wt.% PSf in *N,N*-dimethylformamide (DMF) at  $35^\circ\text{C}$ . Then the coating machine spread the casting solution onto a glass surface in a controlled thickness film. The wet film was precipitated in water bath immediately.

We obtained series of PSf-LS membranes (PSf-LS1, PSf-LS2, PSf-LS3) by changing the LS concentration in the casting solution (1, 2 and 3 wt.%, respectively) and the temperature of the water bath.

The obtained membranes were light yellow color. After precipitation, they were kept in distilled water for a week and were daily rinsed before use.

### 2.2. Membrane characterization

PSf-LS membranes were characterized by reflectance infrared (Bruker-Tensor 27) to demonstrate the incorporation of LS in the membrane.

Cross-section images of PSf blank and PSf-LS membranes were obtained by scanning electron microscopy (SEM, JEOL JSM-6400). The membrane morphologies present in the SEM pictures were analyzed by software IFME<sup>®</sup> [8].

### 2.3. Transport experiments

In our research, we are using flux ( $\text{J mol cm}^{-2} \text{ s}^{-1}$ ) to evaluate the membrane ability for proton and methanol transport. The transport cell includes two compartments, which are separated by the tested membrane [9]. In the case of proton transport, the initial feed was 1.0 M HCl aqueous solution and the stripping was 1.0 M NaCl aqueous solution. The pH value of stripping was measured every 2 s by a Crison Compact Titrator. In the case of methanol transport, the initial feed was 1.0 M methanol aqueous solution and stripping was deionized water. The methanol in the stripping was detected versus time by HPLC (Agilent 1100), using a XDB-C8 column.

Eq. (1) describes permeability coefficient ( $p$ ,  $\text{cm}^3 \text{ cm}^{-2} \text{ s}^{-1}$ ) [10]:

$$-\ln \frac{C_f}{C_0} = \frac{Ap}{V_f} t \quad (1)$$

where  $C_0$  ( $\text{mol l}^{-1}$ ) is the initial concentration of feed,  $C_f$  ( $\text{mol l}^{-1}$ ) is the feed concentration calculated through the stripping solution at time  $t$  (s).  $V_f$  is the feed volume (ml) and  $A$  the actual membrane area ( $\text{cm}^2$ ). From Eq. (1) we observe the linear relationship between  $-\ln(C_f/C_0)$  and time. The slope of the corresponding plot determines the value of  $p$ .

Under steady-state condition, proton and methanol flux were calculated by Fick's First Law:

$$J = \frac{P\Delta C}{l} \quad (2)$$

where,  $l$  (cm) is the membrane thickness.  $\Delta C$  is the concentration difference between the initial feed and the final stripping. In our condition,  $C_0$  is much greater than the final stripping concentration, so we consider  $\Delta C \approx C_0$ .

$P$  is the permeability ( $\text{cm}^2 \text{ s}^{-1}$ ), which is defined as:

$$P = pl \quad (3)$$

Then the flux is related to the permeability coefficient:

$$J = pC_0 \quad (4)$$

Selectivity  $\alpha$  of proton over methanol is a comprehensive evaluation of membranes and is calculated by Eq. (5):

$$\alpha = \frac{J_{\text{H}^+}}{J_{\text{Methanol}}} \quad (5)$$

### 2.4. Impedance spectroscopy

In order to check that the results from transport experiments reflected the intrinsic conductivity of tested membranes, we also measured proton conductivity of some selected hydrated membranes by using impedance spectrometry (Solartron 1260). The cell has two compartments with volume of  $10 \text{ cm}^3$  each, the electrode used was Ag/AgCl. Membranes were examined at maximum voltage of 10 mV with the contact solution of 0.1 M NaCl.

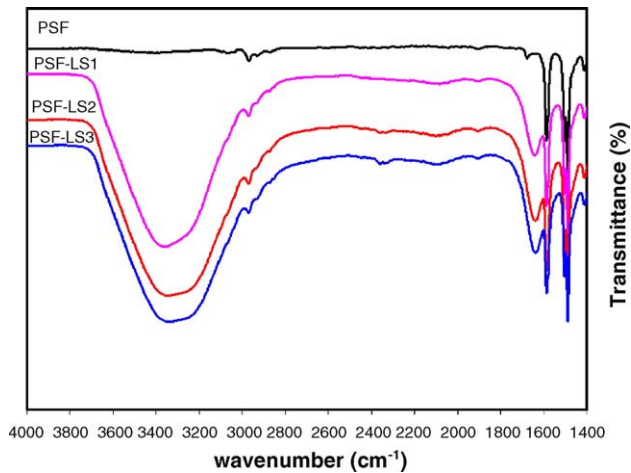


Fig. 2. IR spectra of PSf and PSf-LS membranes.

### 3. Results and discussion

#### 3.1. Reflectance Infrared spectra

Fig. 2 shows the IR spectra of PSf and PSf-LS membranes. Comparing to the spectrum of PSf blank membrane, PSf-LS spectra show absorption peaks at  $3451\text{--}3100\text{ cm}^{-1}$  and

at  $1700\text{--}1600\text{ cm}^{-1}$  which are assigned to O–H stretching vibration and C=O stretching, respectively. They refer to the phenolic hydroxyl groups and carbonyl groups of LS [11]. These IR absorption bands revealed that LS was incorporated into the PSf network.

#### 3.2. Scanning electron microscopy

The cross-sections of membranes were scanned by SEM. Fig. 3 shows cross section images of PSf blank, PSf-LS1, PSf-LS2 and PSf-LS3 membranes obtained at  $20^\circ\text{C}$  of water bath. A clear influence of LS on macrovoid formation can be observed. The membrane with high LS concentration showed morphology with reduced macrovoid. At the same time, higher LS concentration caused the presence of larger pores. Macrovoid formation is a liquid–liquid de-mixing process. Instantaneous de-mixing favors macrovoid formation [12]. Therefore, a possible explanation of the reduction in macrovoid formation is that LS, as an ionic polymer, has a good dispersing property. The interaction between LS and DMF would delay the DMF/water exchange process. The consequence of that delay would be the observed decrease in macrovoid formation and the formation of more open and regular morphologies.

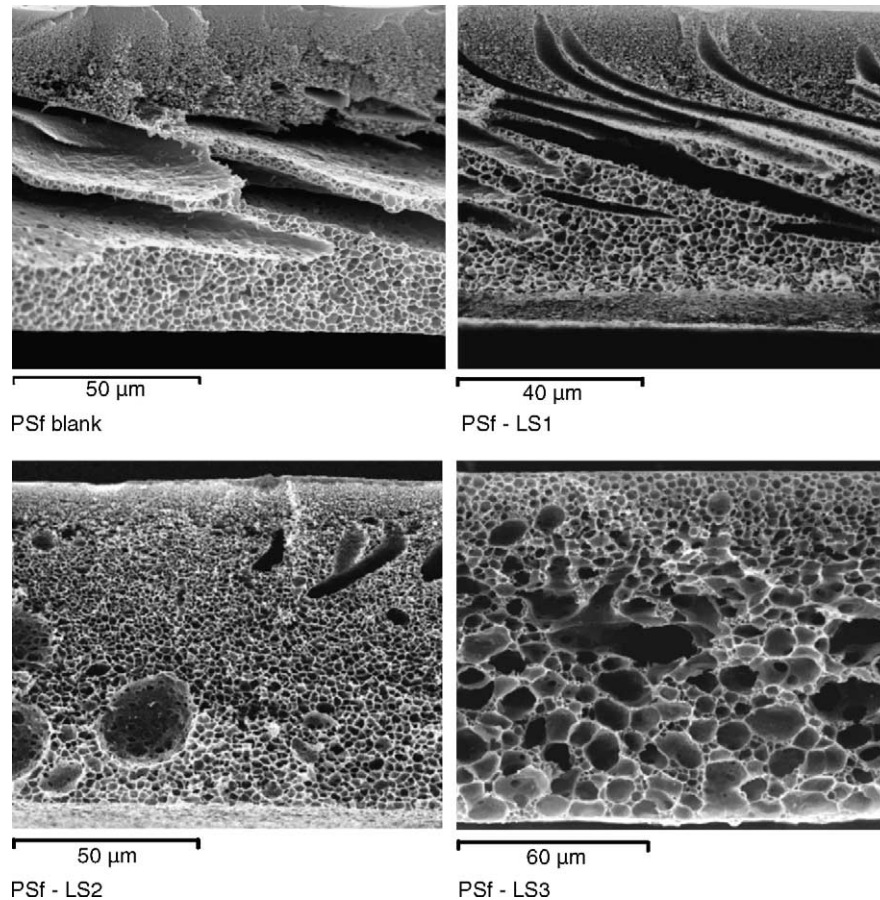


Fig. 3. SEM cross-section images of PSf blank and PSf-LS membranes (precipitated at  $20^\circ\text{C}$ ).

Table 1  
Asymmetry analysis for PSf-LS membranes at two different loads of LS obtained at several precipitation temperatures

	PSf-LS2				PSf-LS3			
	11 °C	15 °C	20 °C	35 °C	11 °C	15 °C	20 °C	35 °C
Asymmetry %	9	11	13	15	7	10	10	16

Precipitation temperature also has an influence on the morphology of the membrane. The asymmetry analysis results are presented in Table 1. A membrane with a homogeneous pore distribution and less macrovoids has a low asymmetry value. We observed that the membrane tended to be more asymmetric when precipitated at high temperature and more macrovoids were formed at higher precipitation temperature. This morphology change could also be a result of the de-mixing process. High precipitation temperature accelerates the solvent–non-solvent diffusion, which speeds up the de-mixing process and results in the presence of more macrovoids.

These morphologies have a direct influence on mass transport resistance. As expected, larger pores and macrovoids drive to lower mass transport resistance.

### 3.3. Proton transport

In the present article, we choose the proton transport ability as the main parameter to be considered, although for specific possible future applications, other considerations might gain importance, like methanol cross-over or hydrogen gas permeability.

Different membranes were investigated such as: PSf blank membranes, PSf-LS membranes and Nafion 117. The permeability for proton through Nafion was determined to be  $5.17 \times 10^{-4} \text{ cm}^3 \text{ cm}^{-2} \text{ s}^{-1}$ , and so the resulting flux was calculated as  $5.17 \times 10^{-7} \text{ mol cm}^{-2} \text{ s}^{-1}$ . This value is used as the reference to compare with those of PSf-LS membranes.

Proton fluxes of PSf-LS membranes calculated from Eqs. (1) and (4) are presented in Fig. 4. These values range from 0.9 to  $5.4 \times 10^{-7} \text{ mol cm}^{-2} \text{ s}^{-1}$ .

We observe that proton fluxes obtained with 1 and 2 wt.% of LS concentration membranes show the same behavior versus precipitation temperature. At these LS compositions 15 °C yields the higher values in proton transport.

We also observe that when LS concentration is 3 wt.%, the proton flux exhibited a different behavior when changing the precipitation temperature. In this case the proton flux continuously increased when increasing the precipitation temperature. This behavior was coincident with the conclusion from SEM images that more macrovoids were observed at higher precipitation temperature. The different behaviors of 1 and 2% membranes to the 3% ones were also evident when analyzing the SEM images.

Finally, at the same precipitate temperature, the proton flux increases when more LS is added to the polymer casting solution. This tendency is clearly due to the facilitated proton transport by acid groups of LS. Under the same conditions,

the proton transport through blank PSf membrane was several orders lower ( $1.53 \times 10^{-12} \text{ mol cm}^{-2} \text{ s}^{-1}$ ) than PSf-LS membranes. While we observe in Fig. 3 that PSf blank membrane and PSf-LS1 have similar morphologies so that the main mechanism of proton transport through PSf-LS membranes cannot be diffusion. We think the facilitated transport mechanism will be responsible for the different transport values although diffusion might have a secondary influence due to the morphology change when larger amounts of LS was added.

### 3.4. Membrane conductivity

Proton conductivity is considered to be the intrinsic property of the membrane and it is conventionally measured by impedance spectroscopy. In order to compare with these reported results, several PSf-LS membranes were tested. For example, PSf-LS3 membranes precipitated at 11 °C were measured by impedance spectrometry and presented an average ion conductivity of  $0.9 \text{ mS cm}^{-1}$ , which is in the acceptable conductivity range for a proton transport membrane [14,15]. The conductivity of Nafion 117 was reported to be  $8.05 \text{ mS cm}^{-1}$  under the same experimental conditions [13].

### 3.5. Methanol transport and membrane selectivity

After the measurements of proton flux, we chose the following five membranes for further measurements: PSf-LS2

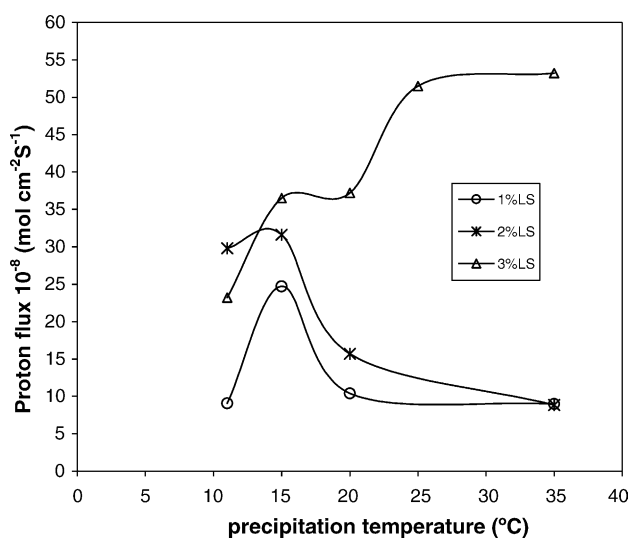


Fig. 4. Proton flux of PSf-LS membranes versus precipitation temperature.

Table 2

Methanol flux through selected PSf-LS membranes obtained at different precipitation temperatures and methanol flux through Nafion 117 as a reference

	PSf-LS2 (11 °C)	PSf-LS2 (15 °C)	PSf-LS3 (20 °C)	PSf-LS3 (25 °C)	PSf-LS3 (35 °C)	Nafion 117
Methanol flux $10^{-7}$ (mol cm $^{-2}$ s $^{-1}$ )	0.347	0.56	0.614	0.719	1.06	1.18

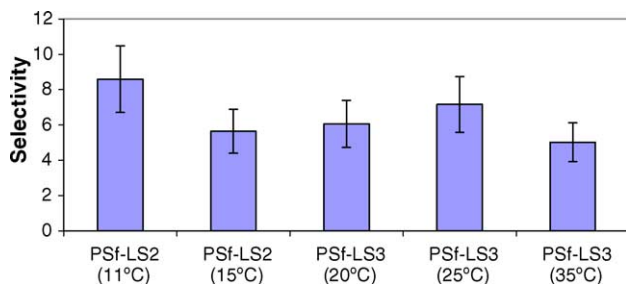


Fig. 5. Selectivity values as proton over methanol for selected PSf-LS membranes obtained at different precipitation temperatures.

precipitated at 11 °C, PSf-LS2 precipitated at 15 °C, PSf-LS3 precipitated at 20 °C, PSf-LS3 precipitated at 25 °C, PSf-LS3 precipitated at 35 °C.

Considering a possible application in DMFC, methanol transport through the membranes is another important factor. Therefore, we measured the methanol flux for the selected membranes precipitated at different temperatures and Nafion 117 under the same measuring condition (25 °C) in order to have a reference value.

Methanol permeability of Nafion 117 calculated by Eqs. (1) and (3) was determined to be  $2.54 \times 10^{-6}$  cm $^{-2}$  s $^{-1}$ , which is very close to the value reported by Pivovar et al. and Won et al. [16,17]. Corresponding methanol flux calculated from Eq. (4) was  $1.18 \times 10^{-7}$  mol cm $^{-2}$  s $^{-1}$ .

Table 2 contains the methanol fluxes obtained with selected PSf-LS membranes.

Methanol flux values observed show the same tendency as that of proton flux. High LS concentration causes an increase in methanol flux. When the LS concentration is the same, high precipitation temperature resulted in high methanol flux due to the open morphology. Comparing to Nafion 117, methanol flux of all the tested membranes is relatively lower. This is due to Nafion's flexible backbone, which causes less resistance for methanol when it swells. On the contrary PSf is an aromatic polymer and LS has an aromatic backbone, so the PSf-LS rigid chains show less methanol transport ability.

Fig. 5 shows the selectivity of all PSf-LS membranes calculated by Eq. (5). PSf-LS2 precipitated at 11 °C shows the highest selectivity value.

#### 4. Conclusions

Reflectance IR revealed that the LS was readily contained in the membrane. Due to its dispersing property, LS presence influenced the membrane morphology. Higher LS concentra-

tion reduced macrovoid and made pores more open so that the mass resistance decreased. Precipitation temperature also has influence on the morphology of the membranes. When LS concentration was 3 wt.%, higher temperature resulted in more macrovoids. When LS concentration was less than 3 wt.%, higher temperature reduced the pore size and made the morphology more asymmetric.

PSf-LS membranes showed proton transport ability due to polyionic structure of LS. Higher LS concentration improved the proton transport, so that the proton is mainly transported by a facilitated mechanism that depends on acid group concentration. Selected PSf-LS membranes showed relatively low methanol transport compared to Nafion 117. Results from impedance conductivity demonstrated that PSf-LS membranes exhibited the intrinsic property of proton transport.

Moreover, since LS is a waste or by-product of pulping industry, PSf-LS membrane would present economical and environmental advantages with respect to membranes made by other polymers.

More investigation on thermal and mechanical properties of PSf-LS membranes are undergoing, and long-term stability will be tested in the future.

#### Acknowledgements

The financial support of the work was provided by Spanish Ministry of Science (projects PPQ2001-1215-C03-01 and PPQ2002-04201-C02) and Rovira i Virgili University.

#### References

- [1] J. Kim, B. Kim, B. Jung, *J. Mem. Sci.* 207 (2002) 129–137.
- [2] N. Carretta, V. Tricoli, E. Picchioni, *J. Mem. Sci.* 166 (2000) 189–197.
- [3] Heinzel, V.M. Barragan, *J. Power Sources* 84 (1999) 70–74.
- [4] R. Gonzalez, E. Reguera, J.M. Figueroa, J.D. Martinez, *J. Appl. Polym. Sci.* 90 (2003) 3965–3972.
- [5] H.H. Tseng, M.Y. Wey, J.C. Chen, *Fuel* 81 (2002) 2407–2416.
- [6] G. Cazacu, M.C. Pascu, L. Profibre, A.I. Kowarski, M. Mihaes, C. Vasile, *Ind. Crops Prod.* 20 (2004) 261–273.
- [7] S. Baumberger, C. Lapiere, B. Monties, D. Lourdin, P. Colonna, *Ind. Crops Prod.* 6 (1997) 253–258.
- [8] C. Torras, IFME<sup>®</sup> Registered Software, 02/2003/3395, Spain.
- [9] R. Garcia-Valls, M. Muñoz, M. Valiente, *Anal. Chim. Acta* 387 (1999) 77.
- [10] M. Mulder, *Basic Principles of Membrane Technology*, 2nd ed., Kluwer Academic Publishers, The Netherlands, 1997, pp. 350–352.
- [11] D. Fengel, G. Wegener, *Wood Chemistry, Ultrastructure, Reactions*, Walter de Gruyter, Berlin, 1984, pp. 157–163.

- [12] M. Mulder, Basic principles of Membrane Technology, 2nd ed., Kluwer Academic publishers, 2003, pp. 138–140.
- [13] G. Pourcelly, P. Sistat, A. Chapotot, C. Gavach, V. Nikonenko, J. Mem. Sci. 110 (1996) 69–78.
- [14] D.S. Kim, H.B. Park, J.W. Rhim, Y.M. Lee, J. Mem. Sci. 240 (2004) 37–48.
- [15] Y. Woo, S.Y. Oh, Y.S. Kang, B. Jung, J. Mem. Sci. 220 (2003) 31–45.
- [16] B.S. Pivovar, Y. Wang, E.L. Cussler, J. Mem. Sci. 154 (1999) 155–162.
- [17] J. Won, S.W. Choi, Y.S. Kang, H.Y. Ha, I.H. Oh, H.S. Kim, K.T. Kim, W.H. Jo, J. Mem. Sci. 214 (2003) 245–257.